

(AGN)²

- 11. Heavy Elements and High-Energy Effects
- 13. Active Galactic Nuclei - Diagnostics and Physics

Week 14
June 03 (Monday), 2024

updated on 06/02 20:18

선광일 (Kwangil Seon)
KASI / UST

11.5 Collisional Excitation of H⁰

- Partially ionized regions in AGNs
 - X-rays can easily penetrate through the H⁺ zone of a nebula and enter the neutral gas behind the hydrogen ionization front.
 - They produce a large partially ionized region which contains H⁰, H⁺, and e⁻.
 - Hence, collisional excitation of neutral atoms can occur, and is observed particularly in [O I] $\lambda\lambda 6300, 6364$, and [N I] $\lambda 5199$.
 - In addition, **collisional excitation of H⁰ by thermal electrons produces strong Ly α emission, and makes a significant contribution to H α .**
 - This process occurs in AGNs.
- Collisional excitation of Ly α
 - **Direct collisional excitation** at low densities
 - ▶ H⁰(1s ²S) + e → H⁰(2p ²P^o) + e with a threshold 10.2 eV ($\sim 1.2 \times 10^5$ K).
 - ▶ The emission coefficient is

$$4\pi j_{\text{Ly}\alpha} = n_e n(\text{H}^0) q_{1^2S, 2^2P^o} h\nu_{\text{Ly}\alpha} \quad \text{where} \quad q_{12} = \frac{8.629 \times 10^{-6}}{T^{1/2}} \frac{\gamma(1,2)}{\omega_1} e^{-\chi/kT}$$

Table 3.16

Effective collision strengths for H I

| T(K) | 1 ² S, 2 ² S | 1 ² S, 2 ² P ^o | 1 ² S, 3 ² S | 1 ² S, 3 ² P ^o | 1 ² S, 3 ² D |
|--------|------------------------------------|---|------------------------------------|---|------------------------------------|
| 10,000 | 0.29 | 0.51 | 0.066 | 0.12 | 0.063 |
| 15,000 | 0.32 | 0.60 | 0.071 | 0.13 | 0.068 |
| 20,000 | 0.35 | 0.69 | 0.077 | 0.14 | 0.073 |

- **Indirect excitation** of Ly α at high densities (cascading following collisional excitation to $n = 3$)

- ▶ The collisional strengths decrease rapidly with increasing principal quantum number n (Table 11.3), and the threshold energy increases with n , making the contribution to Ly α emission from collisional excitation to higher levels, followed by cascading down to 2^2P^o quite small.
- ▶ Every excitation to 3^2S or 3^2D is followed by emission of H α and then Ly α .
However, every excitation to 3^2P^o leads to emission of H α and population of 2^2S , under Case B conditions, which does not emit Ly α .
- ▶ Thus, the collisional-excitation contribution to the Ly α emission coefficient may be written

$$4\pi j_{\text{Ly}\alpha} = n_e n(\text{H}^0) (q_{1^2S, 2^2P} + q_{1^2S, 3^2S} + q_{1^2S, 3^2D} + \dots) h\nu_{\text{Ly}\alpha}$$

- ▶ Table 11.4 show the Ly α emission coefficients for (1) the direct excitation case at low density and (2) the direct + indirect excitation case at high density, together with those due to recombination.
- ▶ Note that including the still smaller contributions of excitation to the levels $n > 4$ would result in further increases in the Ly α .

Table 11.4

L α emission coefficients in partially ionized regions (all in $\text{erg cm}^3 \text{ s}^{-1}$)

| T (K) | Low density $n_e \ll 1.5 \times 10^4 \text{ cm}^{-3}$ | | High density $n_e \gg 1.5 \times 10^4 \text{ cm}^{-3}$ | |
|------------|--|---|---|---|
| | $\frac{4\pi j_{\text{L}\alpha}}{n_e n(\text{H}^0)}$ | $\frac{4\pi j_{\text{L}\alpha}}{n_e n_p}$ | $\frac{4\pi j_{\text{L}\alpha}}{n_e n(\text{H}^0)}$ | $\frac{4\pi j_{\text{L}\alpha}}{n_e n_p}$ |
| 10,000 | 2.56×10^{-24} | 2.87×10^{-24} | 4.46×10^{-24} | 4.25×10^{-24} |
| 12,500 | 2.62×10^{-23} | 2.39×10^{-24} | 4.51×10^{-23} | 3.53×10^{-24} |
| 15,000 | 2.23×10^{-22} | 2.01×10^{-24} | 2.10×10^{-22} | 3.06×10^{-24} |
| 20,000 | 8.89×10^{-22} | 1.51×10^{-24} | 1.46×10^{-21} | 2.34×10^{-24} |

- The recombination emission coefficient of Ly α is given by

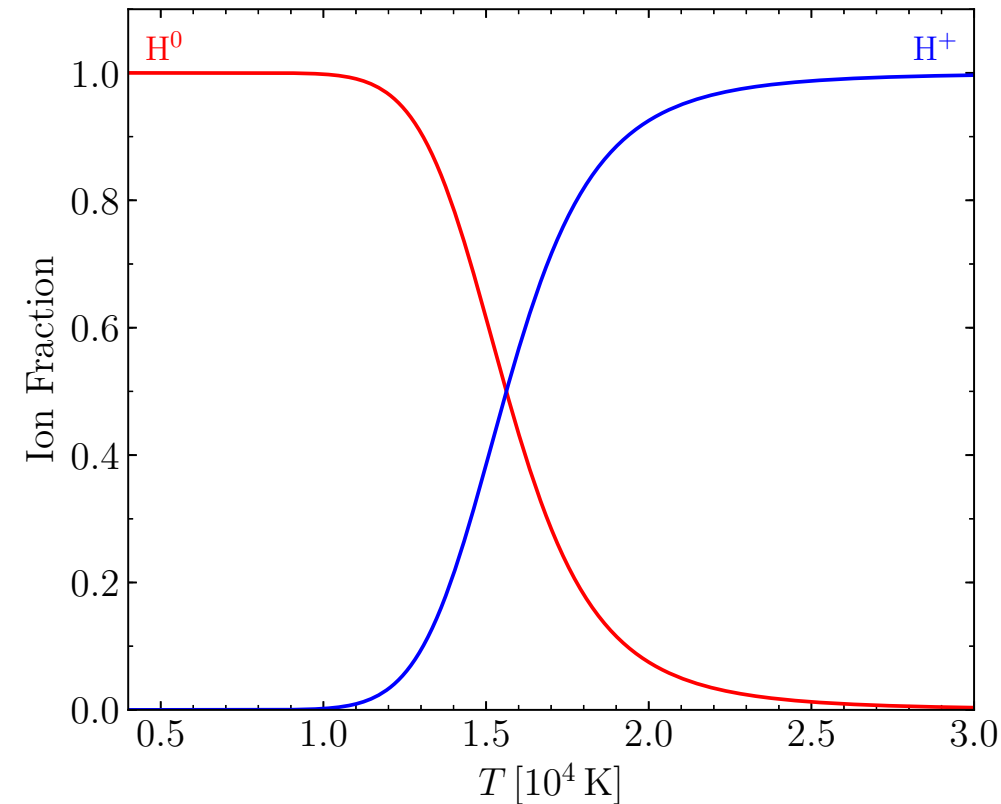
$$\begin{aligned} 4\pi j_{\text{Ly}\alpha} &= n_e n_p \alpha_{2^2P_0}^{\text{eff}} h\nu_{\text{Ly}\alpha} \\ &= n_e n_p (\alpha_B - \alpha_{2^2S}^{\text{eff}}) h\nu_{\text{Ly}\alpha} \end{aligned}$$

Here, numerical values of $\alpha_{2^2S}^{\text{eff}}$ are shown in Table 4.11.

- Collision vs. Recombination

- Note that collisionally excited emission of Ly α increases rapidly with temperature, because of its high threshold (10.2 eV).
- For a half-ionized gas with $n(\text{H}^0) = n_p$:
 - At $T = 10,000$ K, the collisional and recombination contributions to Ly α are roughly the same.
 - At $T = 12,500$ K, the collisional excitations are more important by nearly a factor of ten. However, heating a gas to such a high temperature while maintaining neutrality is nearly impossible.
- For a mostly ionized gas with $n(\text{H}^0) \approx 0.09n_p$:
 - At $T = 12,500$ K, the collisional and recombination contributions to Ly α are approximately equal.

Collisional Ionization Equilibrium



-
- Collisional shift of 2^2S to 2^2P^o at high densities
 - At higher densities, the 2^2S state (resulting from collisional excitation, recombination, or cascading) are collisionally shifted to 2^2P^o and then emit Ly α .
 - The critical density for this process is

$$n_c = \frac{A_{2^2S, 1^2S}}{q_{2^2S, 2^2P^o}^p + q_{2^2S, 2^2P^o}^e} \approx 1.5 \times 10^4 \text{ [cm}^{-3}\text{]} \quad \text{for } n_e \approx n_p.$$

- **Collisional excitation:** Thus, in this high-density limit, the first approximation to the collisional-excitation emission coefficient (including the mixing effect) is

$$4\pi j_{\text{Ly}\alpha}^{\text{coll}} = n_e n(\text{H}^0) (q_{1^2S, 2^2S} + q_{1^2S, 2^2P}) h\nu_{\text{Ly}\alpha}.$$

A better approximation is

$$4\pi j_{\text{Ly}\alpha}^{\text{coll}} = n_e n(\text{H}^0) \sum_{n=2}^3 \sum_{L=0}^{n-1} q_{1^2S, n^2L} h\nu_{\text{Ly}\alpha}$$

- **Recombination:** in high-density limit, the recombination emission coefficients (including the mixing) is

$$4\pi j_{\text{Ly}\alpha}^{\text{rec}} = n_e n_p \alpha_B h\nu_{\text{Ly}\alpha}$$

- Both the collisional and recombination Ly α emission coefficients are larger by factors of ~ 1.5

Table 11.4

$\text{Ly}\alpha$ emission coefficients in partially ionized regions (all in $\text{erg cm}^3 \text{ s}^{-1}$)

| T (K) | Low density $n_e \ll 1.5 \times 10^4 \text{ cm}^{-3}$ | | High density $n_e \gg 1.5 \times 10^4 \text{ cm}^{-3}$ | |
|------------|---|---|---|---|
| | Collisional $\frac{4\pi j_{\text{Ly}\alpha}}{n_e n(\text{H}^0)}$ | Recombination $\frac{4\pi j_{\text{Ly}\alpha}}{n_e n_p}$ | Collisional $\frac{4\pi j_{\text{Ly}\alpha}}{n_e n(\text{H}^0)}$ | Recombination $\frac{4\pi j_{\text{Ly}\alpha}}{n_e n_p}$ |
| 10,000 | 2.56×10^{-24} | 2.87×10^{-24} | 4.46×10^{-24} | 4.25×10^{-24} |
| 12,500 | 2.62×10^{-23} | 2.39×10^{-24} | 4.51×10^{-23} | 3.53×10^{-24} |
| 15,000 | 2.23×10^{-22} | 2.01×10^{-24} | 2.10×10^{-22} | 3.06×10^{-24} |
| 20,000 | 8.89×10^{-22} | 1.51×10^{-24} | 1.46×10^{-21} | 2.34×10^{-24} |

-
- Collisional-excitation emission of H α
 - Collisional excitation to any of the levels 3^2S , 3^2P^o , or 3^2D leads to H α emission under Case B conditions.
 - Thus, the first approximation to the collisional-excitation emission coefficient for H α is

$$4\pi j_{H\alpha} = n_e n_p \sum_{L=0}^2 q_{1^2S, 3^2L} h\nu_{H\alpha}.$$

[Table 11.5] H α emission coefficients in partly ionized regions for $n_e = 10^4 \text{ cm}^{-3}$ (in $\text{erg cm}^{-3} \text{ s}^{-1}$)

| T (K) | Collisional $\frac{4\pi j_{H\alpha}}{n_e n(H^0)}$ | Recombination $\frac{4\pi j_{H\alpha}}{n_e n_p}$ |
|------------|--|---|
| 10,000 | 2.12×10^{-26} | 3.54×10^{-25} |
| 12,500 | 3.47×10^{-25} | 2.89×10^{-25} |
| 15,000 | 2.28×10^{-24} | 2.46×10^{-25} |
| 20,000 | 2.25×10^{-23} | 1.81×10^{-25} |

- Collisional excitation show a stronger temperature dependence.
If $n(H^0) = n_p$ and $T = 10,000 \text{ K}$, the collisional H α emission is about 8% as large as the recombination emission.
If $n(H^0) = 0.11 n_p$ and $T = 12,500 \text{ K}$, the collisional H α emission is about 19% of the recombination contribution.

- Collisional-excitation of H β and higher Balmer lines
 - They are even smaller with respect to the recombination contributions, because of the higher thresholds and smaller cross sections.
 - The degree of ionization of H and the temperature vary strongly as the ionization approaches zero in the transition region of an AGN.
- Therefore, quantitative statements about the total collisionally excited contributions to the various H I line emission depend upon detailed model calculations (as will be discussed in Chapters 13 and 14).
 - In general, (1) the collisionally excited Ly α emission is quite important
 - (2) the collisional excitation adds a small but significant contribution to the H α recombination emission
 - (3) the collisional contributions to H β and higher Balmer lines are nearly negligible.
- From these models, for the entire AGN narrow line region (NLR), **the intrinsic Balmer decrement is approximately H α /H β = 3.1**, which exceeds the recombination value 2.85, resulting from the effects of collisional excitation of H α .

13.1 Introduction

- H II regions
 - H II regions are found in the outer parts of spiral and irregular galaxies, far from the nucleus.
 - The stellar population of the central regions of these galaxies consists almost entirely of old stars, and little ionized gas is apparent.
- There is a very small minority of galaxies with ionized gas in their nuclei that is not associated with O and B stars.
 - Examples are Seyfert galaxies, radio galaxies, quasars, and quasistellar objects, collectively called active galactic nuclei (AGNs).
 - They are rare in space. On average, they are distant and consequently faint.
 - Only in recent decades have they been recognized and studied intensively.
- Understanding AGNs
 - Every spectral band from the radio, FIR, through the optical and UV, to the X-ray and γ -ray regions, has provided information which has helped in understanding these objects.
 - The ionized gas within them emits a prominent emission-line spectrum.
 - The methods of nebular astrophysics have been useful in studying them.
 - The additional physical processes that occur with the high-energy photons which are present in AGNs but absent from H II regions were described in Chapter 11.
 - **However, extensions to high densities, large volumes and hence large optical depths, and high internal velocities are also necessary.**

13.2 Historical Sketch

- Nuclei of galaxies
 - Edward A. Fath (1908, Lick Observatory)
 - ▶ Most of the **nuclei of the “spiral nebulae”** (now known to be galaxies) showed absorption line spectra, resulting from the integrated star light.
 - ▶ But, in the spectrum of the nucleus of NGC 1068, he found six emission lines ($\text{H}\beta$, $[\text{O II}] \lambda 3727$, $[\text{Ne III}] \lambda 3869$, and $[\text{O III}] \lambda\lambda 4363, 4959, 5007$), which are characteristic of gaseous nebulae.
 - V. M. Slipher obtained much better spectra of this same nucleus in 1917.
 - In 1926, Edwin Hubble noted the PN type emission-line spectra of 3 AGNs (NGC 1068, 4051, 4151).
- Seyfert galaxies
 - In 1943, Carl K. Seyfert discovered more galaxies similar to NGC 1068.
 - A very small fraction of galaxies have nuclei whose spectra show many high-ionization emission lines. These nuclei are luminous, and their emission lines are wider than the absorption lines in normal galaxies.
 - Broad emission lines arising in a bright, small nucleus and covering a wide range of ionization defines the class of objects called Seyfert galaxies.
 - They are the most common type of AGNs, but are very rare compared with typical galactic nuclei.

- Radio loud galaxies
 - In 1939 (Grote Reber) and 1946 (Hey et al.), Cygnus A (3C 405) was detected at 160 MHz.
 - Early interferometric observations revealed Cygnus A as a double radio source (Jennison & Gupta 1953).
 - In 1954, Baade & Minkowski optically identified Cygnus A as a faint galaxy with redshift $z = \lambda/\lambda_0 - 1 = 0.057$.
 - ▶ The enormous energy involved was initially explained within a colliding galaxy scenario.
 - The rich emission-line spectrum of Cyg A proved to be very similar to the spectra of Seyfert galaxies.]
 - Other identifications of similar objects quickly followed.
 - The spectra of the small, highly luminous nuclei of many radio galaxies show emission lines which cover a wide range of ionization, and which are wider than the lines in the spectra of normal galaxies.
 - They are rarer in space than the nuclei of Seyfert galaxies, which are typically radio-quiet (but not radio-silent) and are identified by their optical spectra.

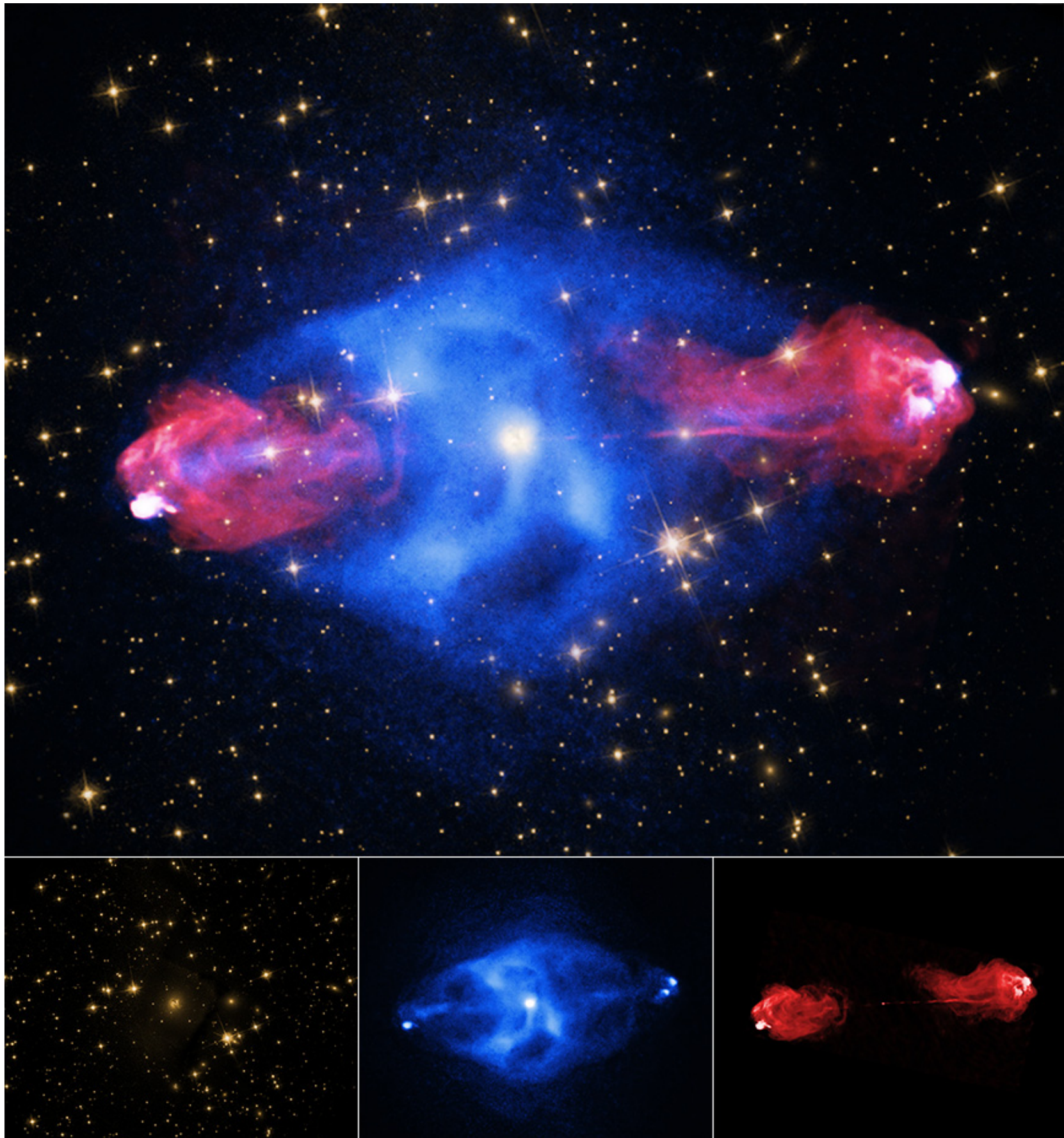
- Quasars
 - A certain fraction of the early optically identified radio sources had no sign of a galaxy or nebula in their images.
 - Their spectra were continuous, with no absorption lines, and with broad emission lines. Initially, they were thought to be stars, perhaps white dwarfs with unusual abundances of some normally rare heavy elements.
 - In 1963, Maarten Schmidth identified several well known nebular emission lines from radio source 3C 273 with the then unusually large redshift $z = 0.158$.
 - Soon after (in 1963), Jesse L. Greenstein identified similar lines in 3C 48, with redshift $z = 0.367$.
 - They are not stars, but quasistellar radio sources, commonly called quasars for short.
 - They are so luminous and so distant that the galaxy in which they are located cannot, or could not, be detected on photographic plates.
 - With CCDs, which reach faint light levels, the stellar-appearing nucleus can be subtracted with good precision, and for many quasars the galaxy has been revealed.
- Quasistellar objects (QSOs)
 - Radio-quiet high-luminosity stellar-appearing objects were found soon afterward.
 - Initially they were called “quasistellar objects” (QSOs) by most researchers, but at present they are commonly referred to as quasars, even though they are radio-quiet.

- They are the most distant objects we known in the universe.
 - From the bright apparent magnitudes of quasars, they are beacons that can be observed out to the distant reaches of the universe.
 - There appears to be a cutoff at redshifts larger than $z \approx 2$, so there are relatively few known with $z > 4$.
 - All quasars and QSOs do not have the same absolute magnitude.
 - Table 13.1 shows the space densities of quasars, Seyfert and radio galaxies.
 - Note that
- $$\# \text{ of quasars} / \# \text{ of radio galaxies} \approx \# \text{ of QSOs} / \# \text{ of Seyfert galaxies}$$
- This seems to indicate that the radio-loud and radio-quiet objets each form physically continuous sequences, covering a wide range of luminosities, much as stars do.
 - The quasars and QSOs represent the rarest but most luminous forms of AGNs.
 - The radio and Seyfert galaxies are more common in space, but less luminous.
- Recent observations found that
 - Almost every galaxy hosts a black hole, but only 1% is active and 99% is silent.
 - About 15-20% of AGNs is radio-loud (Urry & Padovani 1995).
 - Radio-loud AGNs lie in ellipticals, while radio-quiet AGNs lie in spirals and ellipticals.
 - Many AGNs are now thought to be partially obscured by dusty interstellar matters. X-rays are better able to pass through this material than visible light, so surveys at X-rays have fewer observational selection effects.

[Table 13.1] Approximate space densities here and now

| Type | Number Mpc^{-3} | Local Space Densities of Some Objects | |
|---|-----------------------------|--|-----------------|
| | | <i>Object</i> | Gpc^3 |
| Field galaxies | 10^{-1} | Spiral Galaxies $M_v < -20$ | 5×10^6 |
| Luminous galaxies | 10^{-2} | $M_v < -22$ | 3×10^5 |
| Seyfert galaxies | 10^{-4} | $M_v < -23$ | 3×10^3 |
| Radio galaxies | 10^{-6} | Elliptical Galaxies $M_v < -20$ | 1×10^6 |
| QSOs | 10^{-7} | $M_v < -22$ | 1×10^5 |
| Quasars | 10^{-9} | $M_v < -23$ | 10^4 |
| Rich Clusters of Galaxies | | | |
| Radio Galaxies | | | |
| Radio Quasars | | | |
| Radio Quiet Quasars | | | |
| Sy 1 | | | |
| Sy 2 | | | |
| BL Lac | | | |
| Strong IRAS Galaxies | | | |
| Active Galactic Nuclei (Saas-Fee Advanced Course; Blandford, Netzer, Woltjer) | | | |

Cygnus A



A multi-wavelength view of the galaxy in Cygnus A. In the top, composite image, optical data from the Hubble Space Telescope are represented by gold, while X-ray (Chandra) and radio (VLA) data are shown in blue and red respectively. The bottom three panels show the individual images of the composite. Image Credit: X-ray: NASA/CXC/SAO; Optical: NASA/STScI; Radio: NSF/NRAO/AUI/VLA

Fornax A



Fornax A is a galaxy with a very active black hole in its core that is spraying radio waves out into enormous jets. Here, the white glow in the center is the visible galaxy NGC 1316 that you can see through the constellation of Fornax. Notice the wee spiral galaxy above it? These two galaxies are merging, and as gas and dust are stripped out of the small galaxy and poured into the center of NGC 1316, the black hole nestled there spins it up. How do we know this? The huge radio lobes to either side of this merger are the telltale signs that a black hole is being fed more than it can handle. These are the billowing ends of powerful jets shooting out spun-up, escaped material far into space.

Credit: NRAO/AUI/NSF, observers Ed Fomalont (NRAO), Ron Ekers (ATNF), Wil van Breugel (UC-Berkeley), Kate Ebneter (UC-Berkeley)

13.3 Observational Classification of AGNs

- The Sloan Digital Sky Survey (SDSS) have obtained spectra of large portions of the sky and these spectra contain many thousands of AGNs.
- Classification of Seyfert galaxies
 - Seyferts can be classified into two types, following a scheme proposed by E. Khachikian & D. W. Weedman.
 - **Seyfert 1** galaxies have very broad H I, He I, and He II emission lines with FWHM of $\approx 1 - 5 \times 10^3 \text{ km s}^{-1}$, while their forbidden lines ($[\text{O III}] \lambda\lambda 4959, 5007$, $[\text{N II}] \lambda\lambda 6548, 6583$, and $[\text{S II}] \lambda\lambda 6716, 6731$) have FWHMs of $\approx 5 \times 10^2 \text{ km s}^{-1}$.
 - ▶ The forbidden lines are narrower than the very broad permitted emission lines, but they are broader than the emission lines in most starburst galaxies.
 - **Seyfert 2** galaxies have permitted and forbidden lines with approximately the same FWHMs, typically 500 km s^{-1} , similar to the FWHMs of the forbidden lines in Seyfert 1 galaxies.

A spectrophotometric atlas of galaxies (Kennicutt, 1992, ApJS, 79, 255)

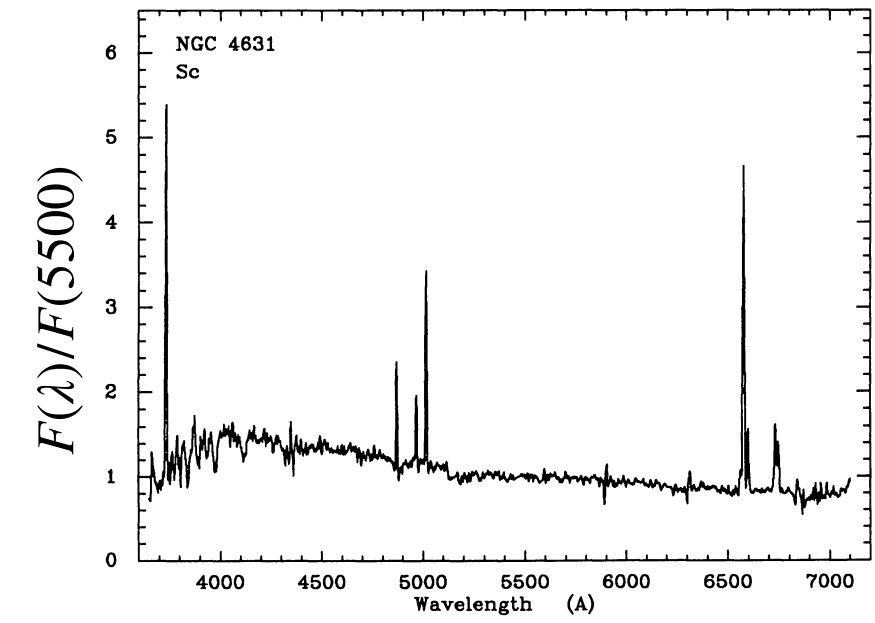
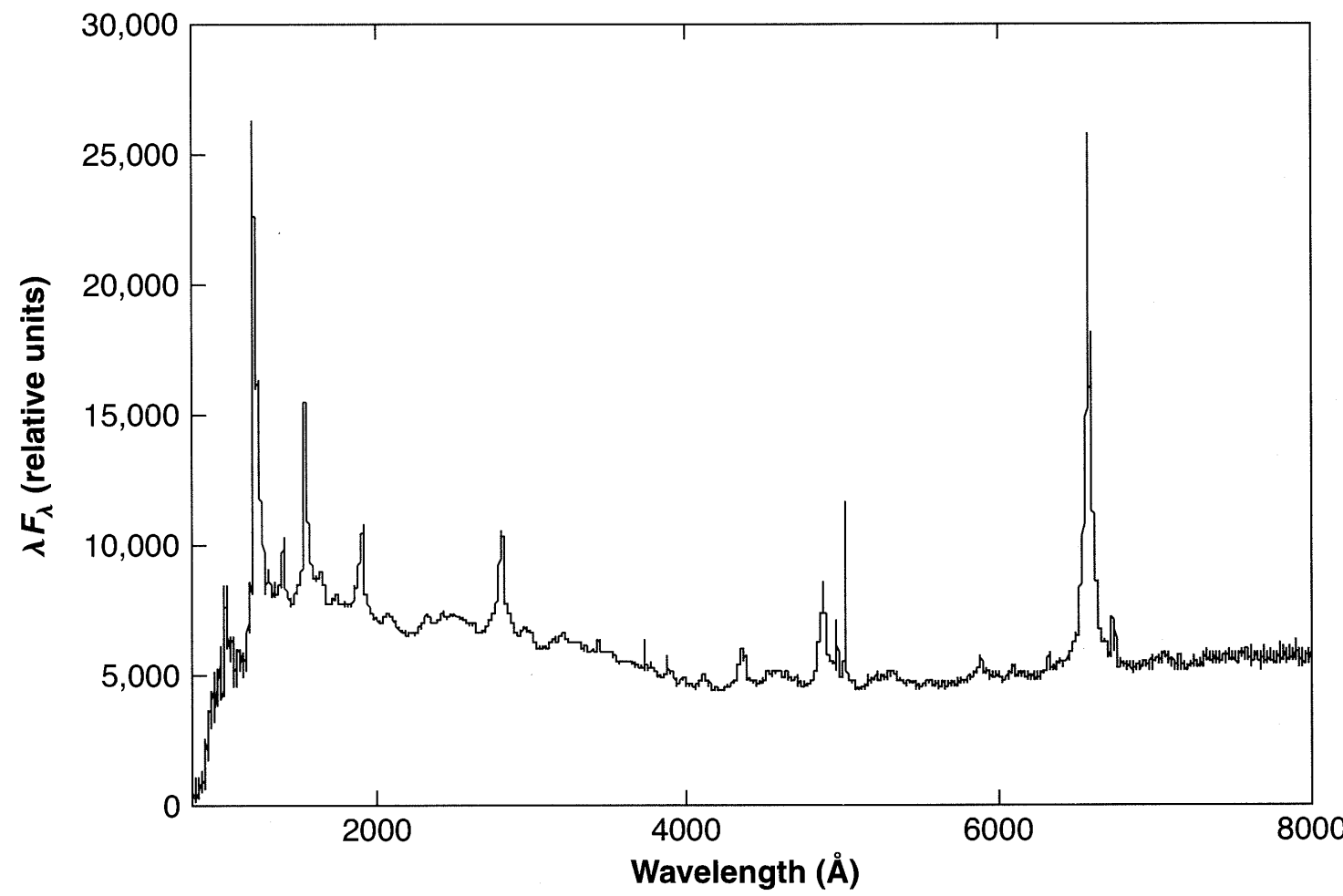
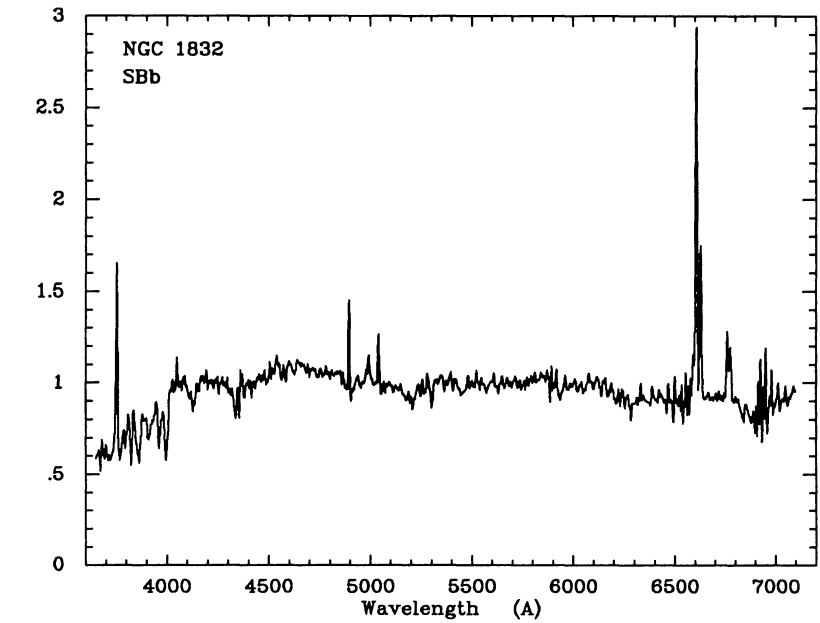
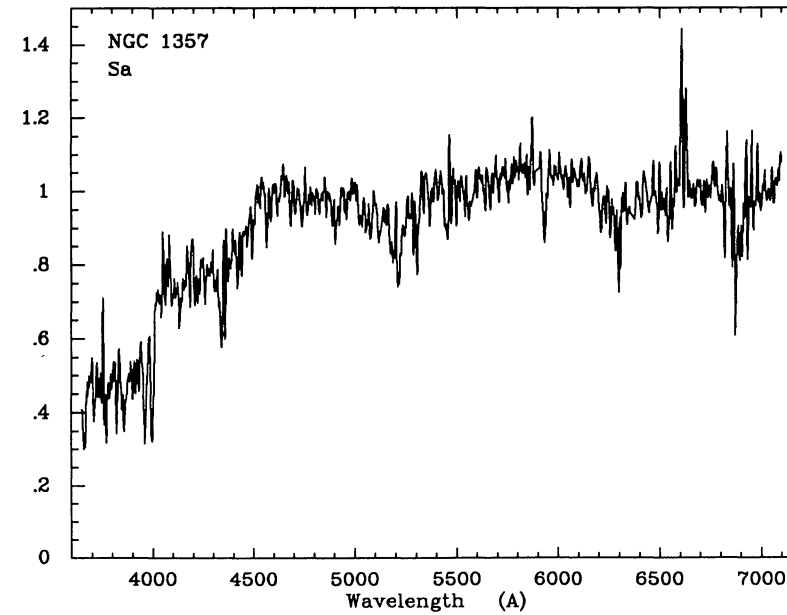
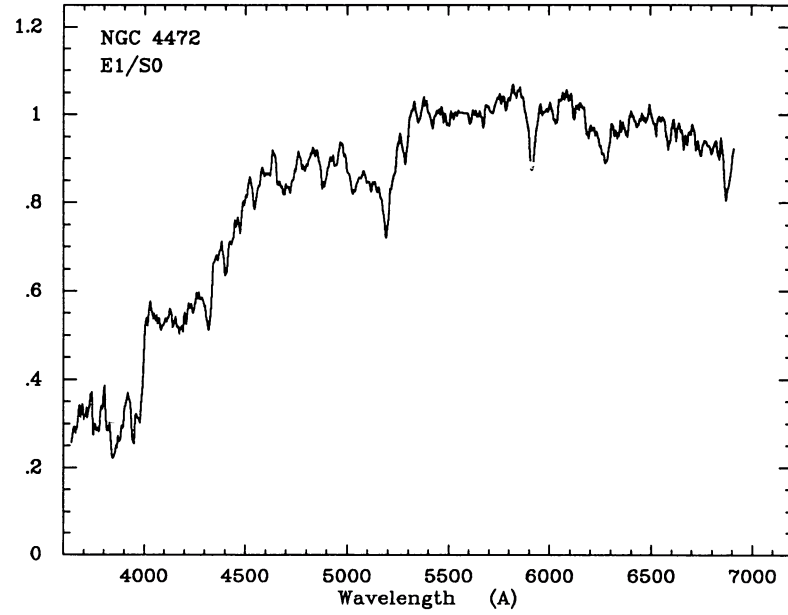
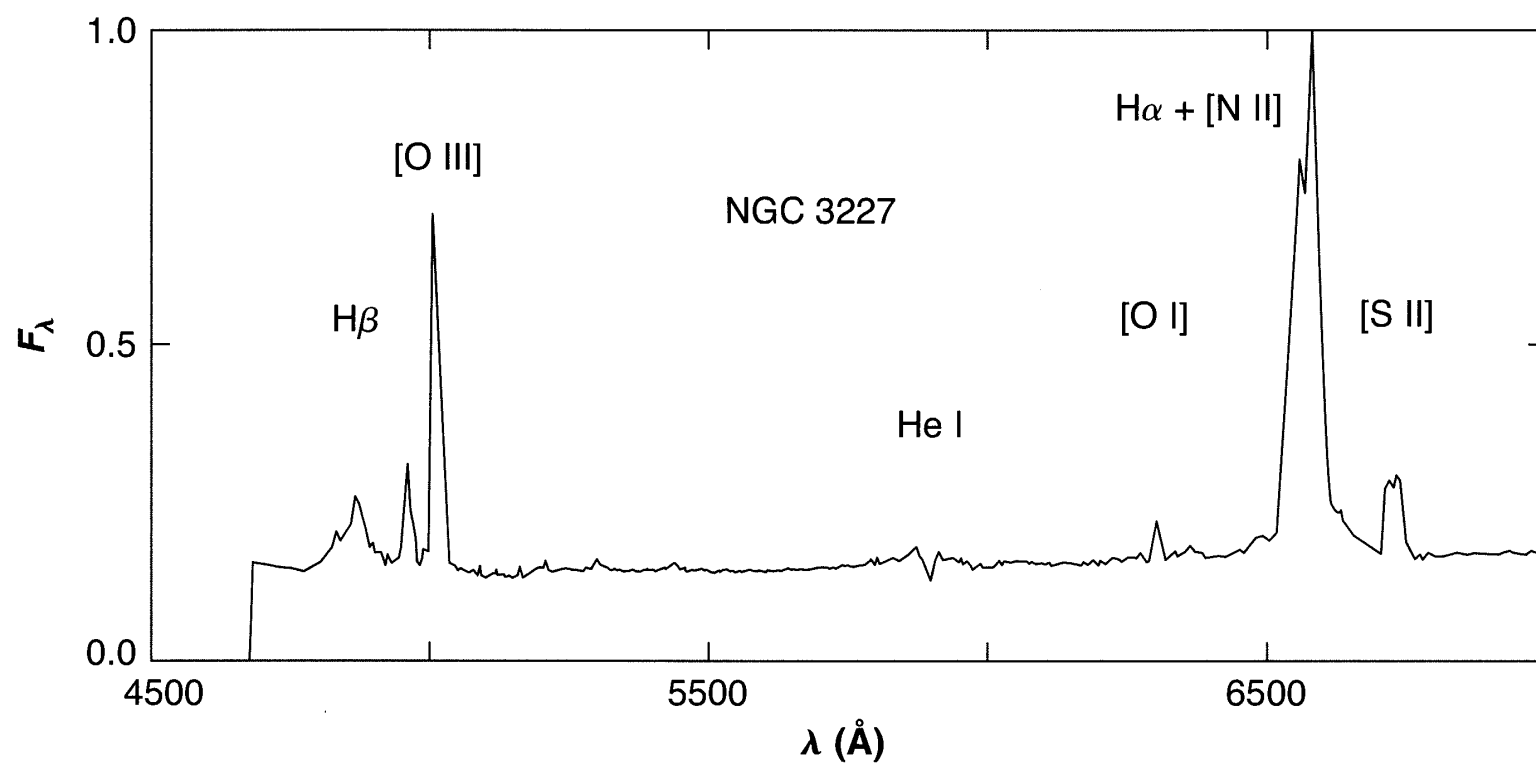
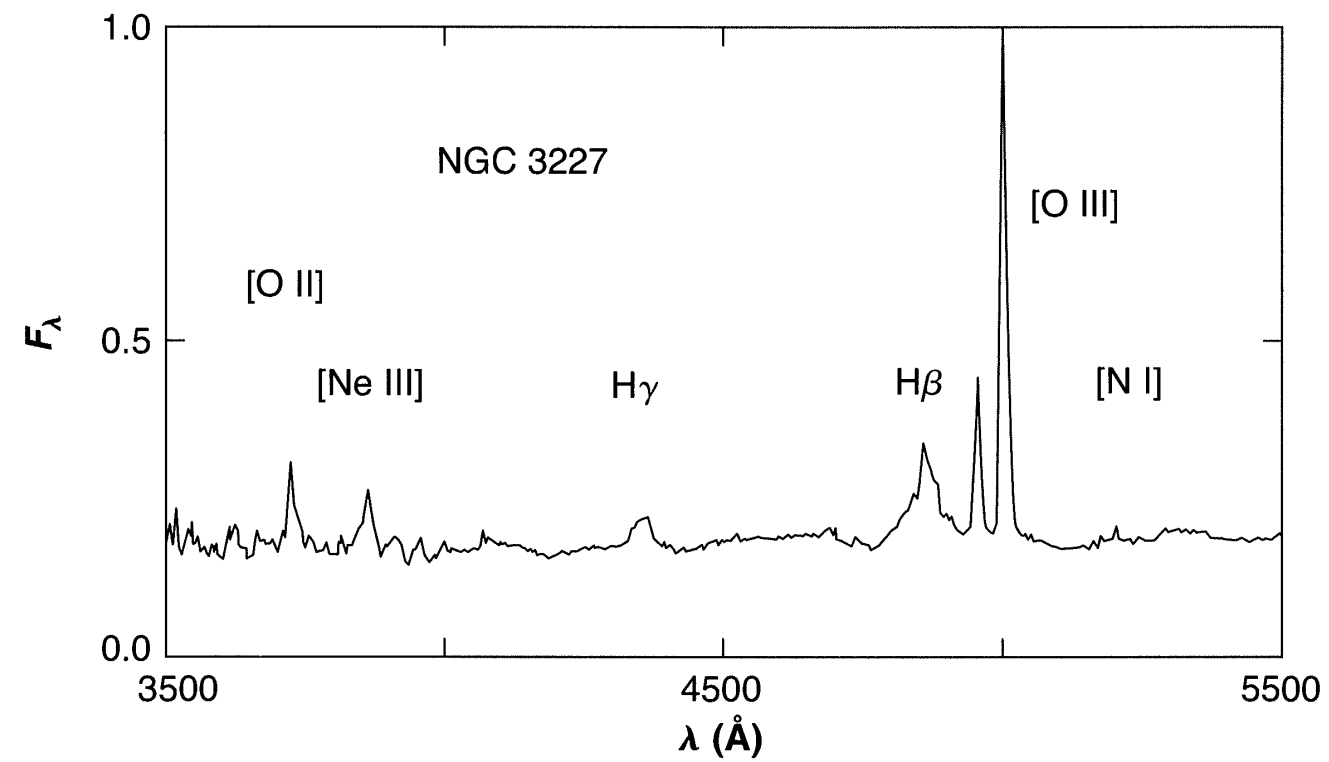
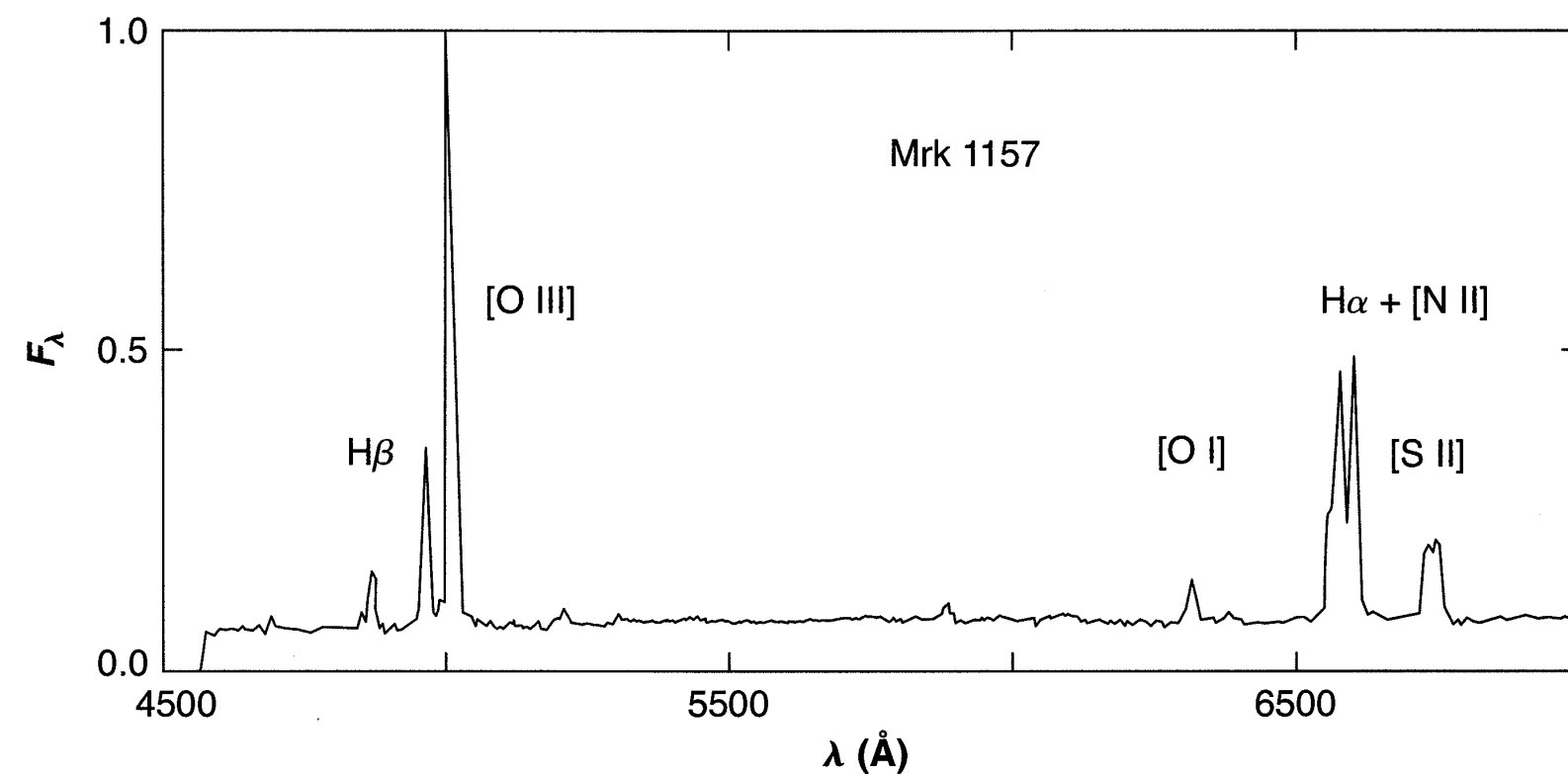
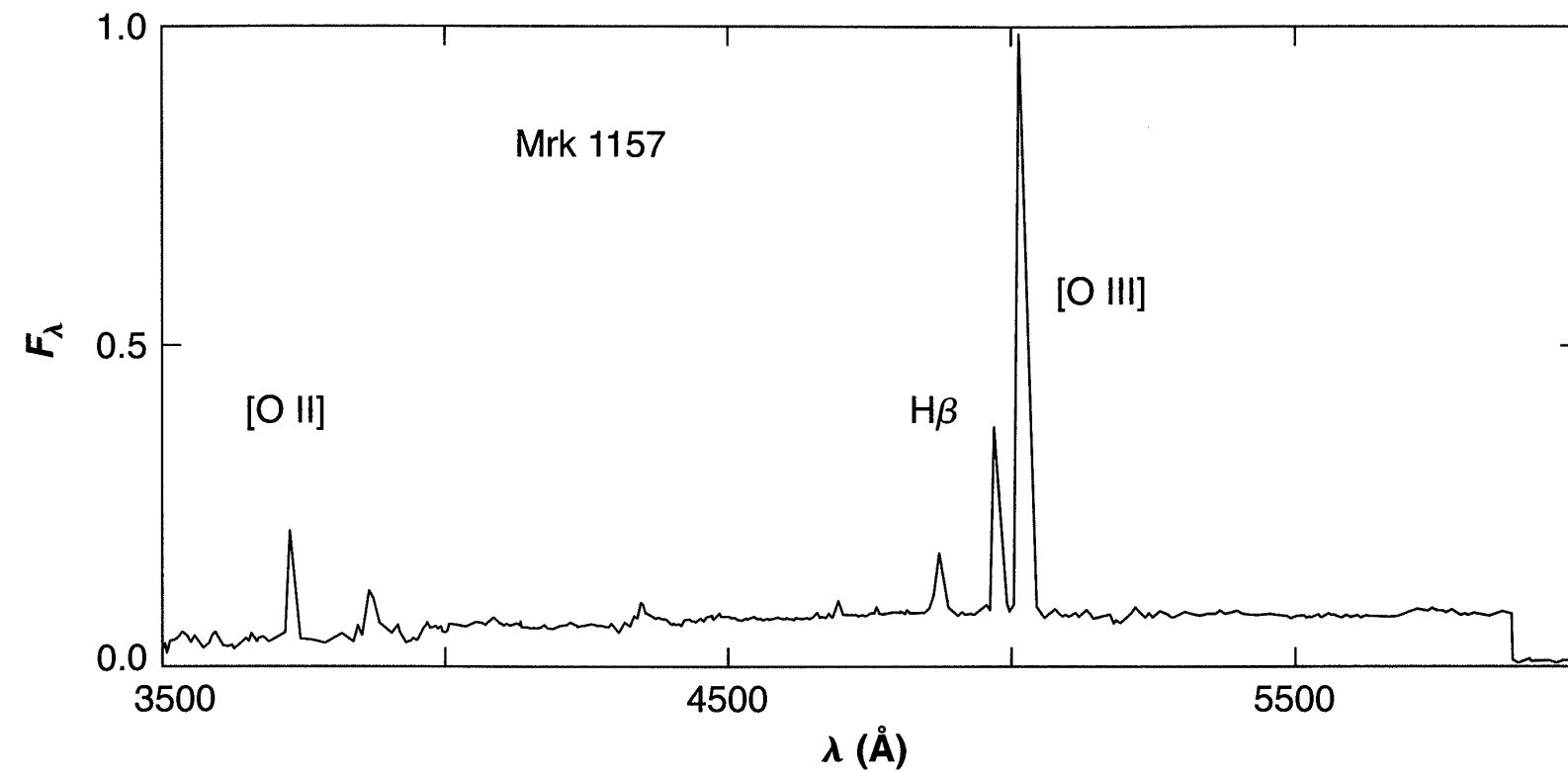


[Figure 13.1]
The composite UV-optical active
nucleus spectrum from the SDSS.

-
- [Figure 13.2] Optical spectrum of a Seyfert 1 galaxy, NGC 3227.



-
- [Figure 13.3] Optical spectrum of a Seyfert 2 galaxy, Mrk 1157



- Subdivision of Seyfert galaxies
 - **Seyfert 1.5 galaxies** have H I emission-line profiles that can be described as composite, consisting of a broad component (like a Seyfert 1), on which a narrower component (as in a Seyfert 2) is superimposed.
 - **Seyfert 1.8 galaxies** have strong narrow components and very weak but still visible broad components of H α and H β .
 - **Seyfert 1.9 galaxies** shows a weak broad component at H α , but none at H β .

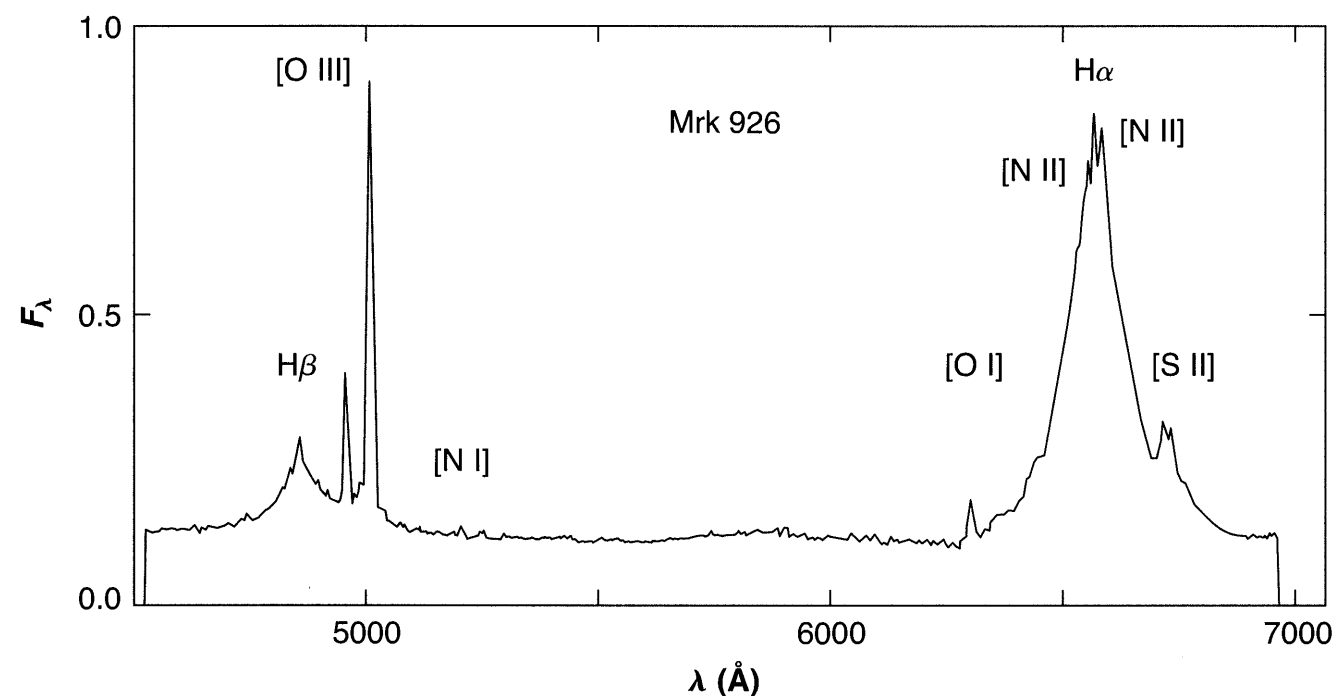
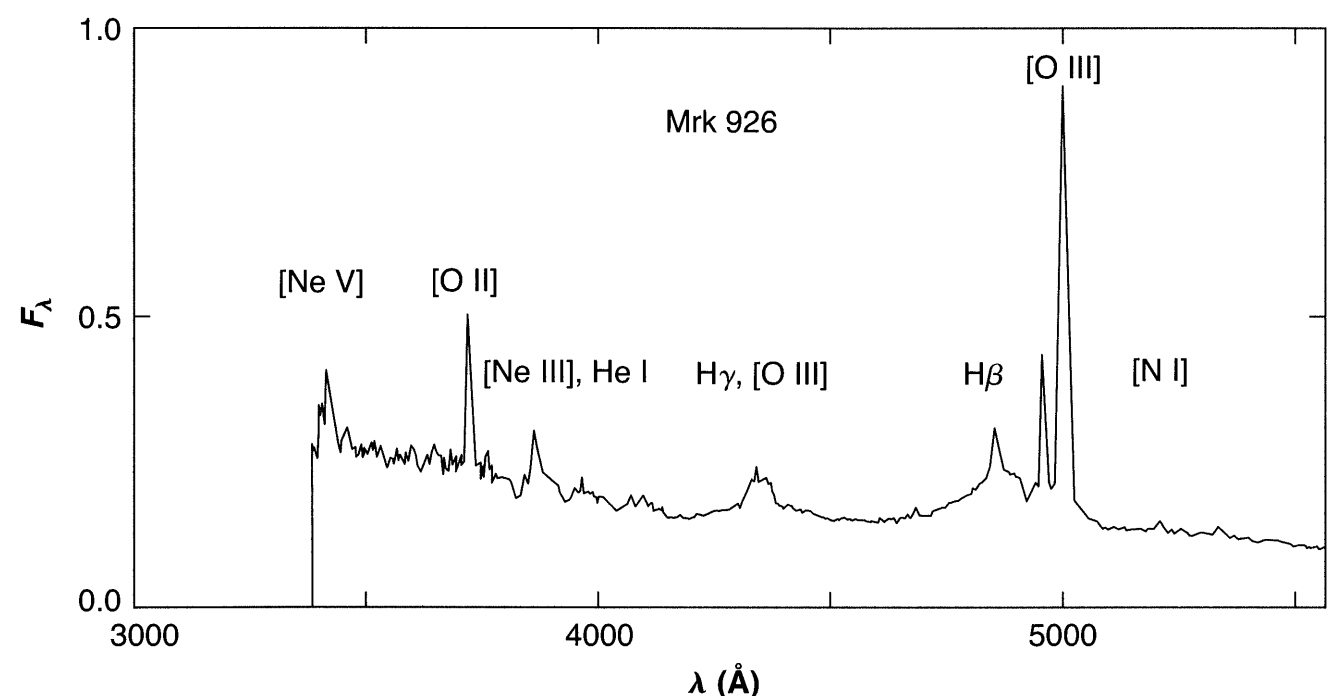


[Figure 13.4] Optical spectrum of Mrk 926, a Seyfert 1.5 galaxy

- Radio loud galaxies vs Radio quiet galaxies
 - **Radio-loud:** the synchrotron radio emission comes from two large lobes, far outside the boundaries of the optical image. In a few case, very faint optical emission has been detected in the radio lobes.
 - **Radio-quiet:** Frequently, there is a weak, compact (flat radio-frequency spectrum) radio source in the nucleus of the galaxy. Strong optical emission + featureless continuum spectrum come from this type of AGNs.
- The optical spectra of radio loud galaxies
 - Broadline Radio Galaxies (BLRGs): Radio-loud equivalent of a Seyfert 1, with broad H I, He I, and He II emission lines but narrower forbidden lines.
 - ▶ An examples i 3C 390.e
 - Narrowline Radio Galaxies (NLRGs): have “narrow” permitted and forbidden lines, similar to Seyfert 2 galaxies.
 - ▶ The best known example is Cyg A (3C 405), the first identified radio galaxy.

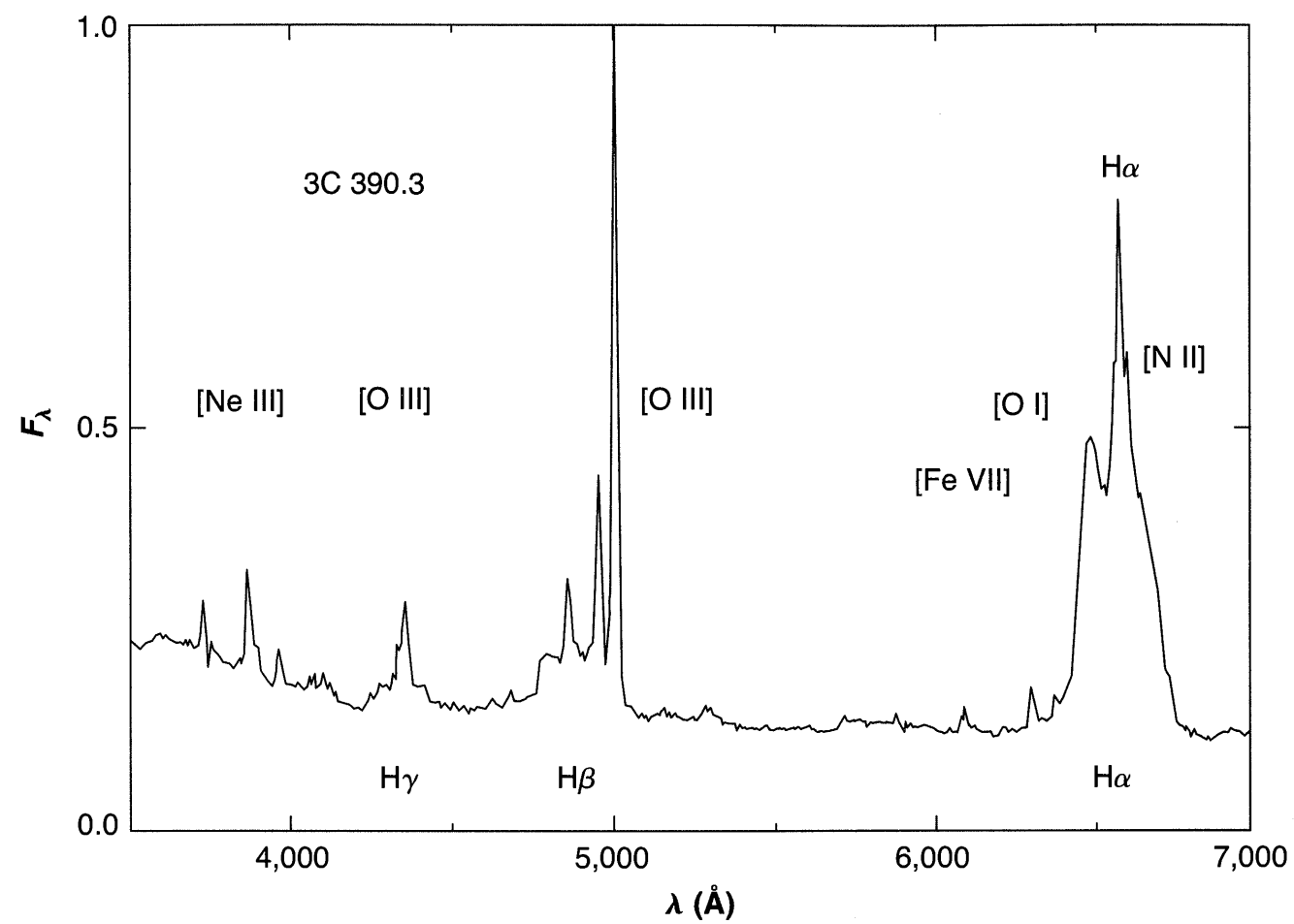


[Figure 13.6]
Optical spectrum of 3C 390.3, a BLRG.

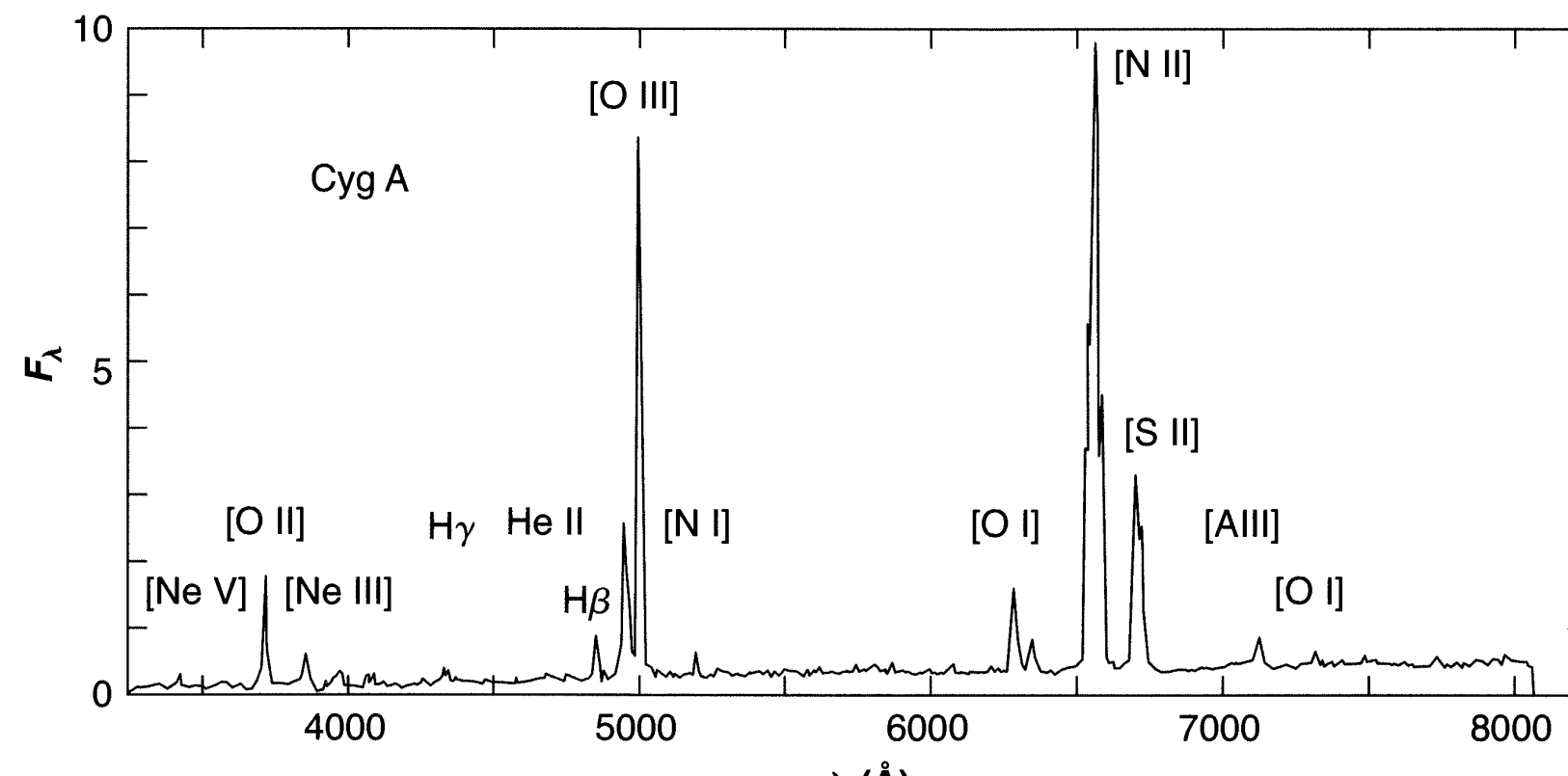


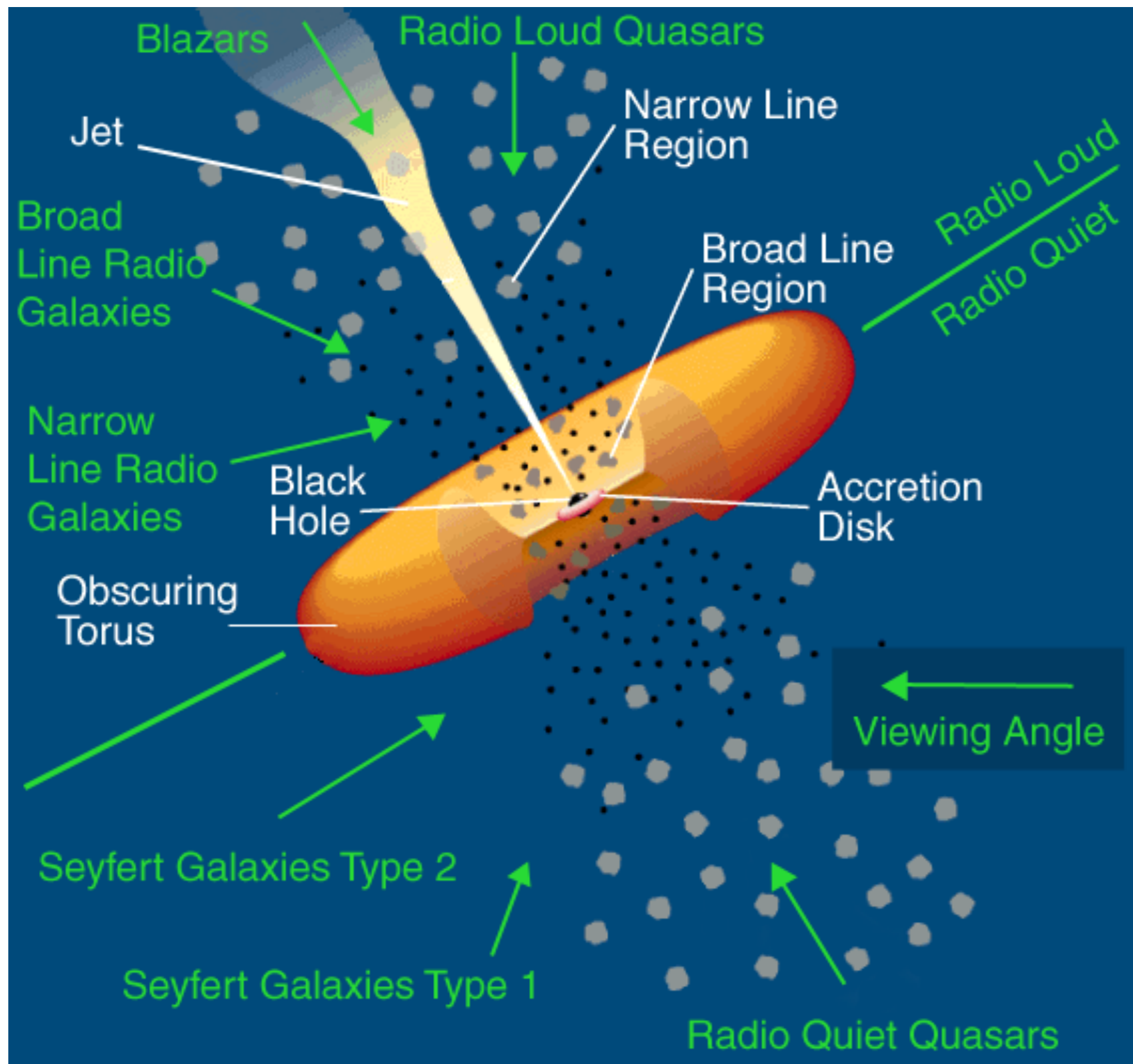
[Figure 13.6]
Optical spectrum of Cyg A, a NLRG.

- Difference between BLRGs and Seyfert 1 AGNs
 - They are similar, but there are some difference between spectra and radio and Seyfert galaxies.
 - BLRGs have composite H I profile, similar to Seyfert 1.5.

Their broad components are typically broader than in “normal” Seyfert 1s, and often are more nearly square shaped, or flat topped, as well as more irregular, or structured.
 - Seyfert 1 AGNs shows broad permitted Fe II emission lines, coming from several strong multiplets of Fe II. They overlap in two broad “bands” near λ 4570 and λ 5250.
 - ▶ These features are relatively weak in NGC 3227 (Figure 13.2), but quite strong in Mrk 376 (Figure 16.4). Other Seyfert 1 spectra show the Fe II line strengths between these two extremes.
- Differences between NLRGs and Seyfert 2s are much smaller, if they exist at all.

- Locations & morphological types
 - All Seyfert galaxies are close enough to use in space and classified as to spirals.
 - ▶ Most are closer to Sb type. Many are barred spirals (SBb).
 - ▶ Many have “companion” galaxies, or galaxies close enough to be interacting gravitationally with them.
 - Almost all of the strong radio galaxies are ellipticals.
 - ▶ Most of the NLRGs are classified as “giant ellipticals” of types cD, D, or E.
 - ▶ All of the BLRGs are morphologically classified as type N, systems with brilliant “star-like” nuclei containing most of the luminosity, but with faint, barely visible “fuzzy” envelopes associated with them. (Thus, N galaxies are nearly quasars.)
- Interstellar matter
 - Spiral galaxies contain more interstellar matter than giant ellipticals, and they are more condensed to their disk planes.
 - The difference between a Seyfert and a radio galaxy may be due to the difference in the near-nuclear environment.
 - A seyfert galaxy has a flattened, rotating, interstellar-matter-rich one.
 - A radio galaxy has a more nearly spherical interstellar-matter-poor one.

- A featureless continuous spectrum + emission lines in the optical region
 - The featureless continuum comes from a tiny, unresolved object (supermassive blackhole) within the nucleus.
 - The featureless continuum is very strong in Seyfert 1 galaxies, often so much stronger than the integrated stellar absorption-line spectrum as to make it nearly invisible. **The light of the AGN completely dominates the total light of the galaxy.**
 - In Seyfert 2 galaxies, the featureless continuum is generally much fainter. In many cases, it can only be detected by careful subtraction of the galactic stellar continuum.
 - The broad emission lines are closely associated with the featureless continuum.
 - The AGNs of Seyfert 1 galaxies are generally more luminous than the AGNs of Seyfert 2s, probably due to the additional light from the nucleus in the Seyfert galaxy.
 - The luminosity function of Seyfert 1 galaxies has its maximum near $M_B = -21$, while for Seyfert 2 galaxies it is near $M_B = -20$.
- Quasars and QSOs
 - Observation data show convincingly that they are simply the rarest and most luminous AGNs.
 - The luminosity function of Seyfert 1 galaxies fits smoothly onto the luminosity function of QSOs (optically selected quasars) around absolute magnitude $M_B = -21$ or -22 .
 - Nearly all galaxies more luminous than about $M_B \approx -22$ contains AGNs.
 - Practically, all known quasars and QSOs are of the BLRG or Seyfert 1 type.
 - Radio-loud quasars seem to be the extension to high optical luminosity of the BLRGs.



13.4 Densities and Temperatures in the Narrow-Line Gas

- The “narrow” emission lines observed in Seyfert 2 and narrow-line radio galaxies
 - They are much the same as those observed in H II regions and planetary nebulae, except that in the AGNs the range of ionization is considerably greater.
 - Not only [O II], [O III], [N II], [Ne III] are observed, but also [O I], [N I], [Ne V], [Fe VIII], [Fe X].
 - [S II], which is relatively low stage of ionization (10.4 eV), is generally much stronger in the AGNs.
 - Permitted lines of H I, He I, and He II are moderately strong.
 - These narrow lines are emitted by highly-ionized gas, with roughly “normal” abundances of the elements.
 - The standard nebular diagnostic methods may be used to analyze it.
- NLRG Cyg A
 - is a particularly well-studied example. Table 13.2 shows its measured line intensities.
 - The measured H I Balmer-line relative strengths do not fit the recombination predictions. The observed Balmer decrement is steeper than the calculated recombination decrement, just as it is in H II regions.

-
- Extinction - Balmer decrement
 - was calculated from the Balmer decrement, to give the best overall fit with the recombination decrement for $T = 10^4 \text{ K}$, $n_e = 10^4 \text{ cm}^{-3}$.
 - The result is $E(B - V) = 0.69 \pm 0.04$, using the standard reddening law.

More weight has been given to the $\text{H}\gamma/\text{H}\beta$ and $\text{H}\delta/\text{H}\beta$ ratios.

The dust extinction corrected value of $\text{H}\alpha/\text{H}\beta$ is 3.08, slightly larger than the recombination value of 2.85.

This increase is real; it results from a **contribution due to collisional excitation of $\text{H}\alpha$** (Section 11.5).

- Cyg A is near the galactic equator in the sky. Therefore, some of $E(B - V)$ is due to dust within our Galaxy. Observations of elliptical galaxies near Cyg A indicate that about half its extinction arises within our Galaxy, and the other half in Cyg A itself.

Observed and calculated relative line fluxes in Cyg A

| Ion | λ (Å) | Relative Fluxes | | Crab Nebula | Photoionization Model |
|------------------|------------------|-----------------|-----------|----------------|--------------------------|
| | | Measured | Corrected | | |
| $\text{H}\delta$ | 4101 | 0.17 | 0.28 | 0.31 | 0.26 |
| $\text{H}\gamma$ | 4340 | 0.32 | 0.46 | 0.61 | 0.47 |
| $\text{H}\beta$ | 1.00 | 1.00 | 1.00 | 1.00 | 1.00 |
| $\text{H}\alpha$ | 6563 | 6.61 | 3.08 | 3.28 | 2.85 |

Table 13.2
Observed and calculated relative line fluxes in Cyg A

| Ion | λ (Å) | Relative Fluxes | | Crab Nebula | Photoionization Model |
|------------|------------------|-----------------|-------------|----------------|--------------------------|
| | | Measured | Corrected | | |
| [Ne V] | 3346 | 0.14 | 0.38 | — | 0.12 |
| [Ne V] | 3426 | 0.36 | 0.95 | 0.46 | 0.34 |
| [O II] | 3727 | 2.44 | 5.00 | 10.3 | 0.24 |
| [Ne III] | 3869 | 0.66 | 1.23 | 1.56 | 0.53 |
| [Ne III] | 3967 | 0.22 | 0.40 | 0.47 | 0.16 |
| [S II] | 4072 | 0.14 | 0.23 | 0.31 | |
| H δ | 4101 | 0.17 | 0.28 | 0.31 | 0.26 |
| H γ | 4340 | 0.32 | 0.46 | 0.61 | 0.47 |
| [O III] | 4363 | 0.16 | 0.21 | 0.19 | 0.19 |
| He I | 4471 | ≤ 0.07 | ≤ 0.09 | 0.28 | 0.02 |
| He II | 4686 | 0.25 | 0.28 | 0.53 | 0.18 |
| H β | 1.00 | 1.00 | 1.00 | 1.00 | 1.00 |
| [O III] | 4959 | 4.08 | 3.88 | 2.81 | 6.3 |
| [O III] | 5007 | 13.11 | 12.30 | 8.43 | 18.1 |
| [N I] | 5199 | 0.40 | 0.32 | — | — |
| [Fe XIV] | 5303 | ≤ 0.10 | ≤ 0.08 | — | 0.01 |
| [Fe VII] | 5721 | ≤ 0.10 | ≤ 0.06 | — | 0.03 |
| [N II] | 5755 | 0.14 | 0.09 | 0.11 | — |
| He I | 5876 | 0.13 | 0.08 | 0.79 | 0.06 |
| [Fe VII] | 6087 | ≤ 0.07 | ≤ 0.04 | — | 0.04 |
| [O I] | 6300 | 2.10 | 1.10 | 1.20 | 1.24 |
| [O I] | 6364 | 0.69 | 0.35 | 0.33 | 0.41 |
| [Fe X] | 6375 | 0.10 | 0.05 | — | 0.07 |
| [N II] | 6548 | 3.94 | 1.90 | 1.56 | 0.29 |
| H α | 6563 | 6.61 | 3.08 | 3.28 | 2.85 |
| [N II] | 6583 | 13.07 | 6.15 | 4.69 | 0.86 |
| [S II] | 6716 | 3.65 | 1.66 | 5.00 | |
| [S II] | 6731 | 3.29 | 1.51 | — | |
| [Ar III] | 7136 | 0.64 | 0.25 | 0.38 | — |
| [O II] | 7325 | 0.35 | 0.13 | 0.50 | — |
| [Ar III] | 7751 | 0.13 | 0.043 | — | — |

- Using one mean extinction law is an extreme oversimplification.
 - Optical properties
 - ▶ The Balmer-line method used to correct the measured line intensities of the spectra of H II regions in other galaxies, starburst galaxy nuclei, and AGNs is the same as the one applied in our Galaxy.
 - ▶ The extinction law has been derived from our Galaxy within approximately 1 kpc of the Sun.
 - ▶ The properties of the dust would no doubt depend on the physical conditions and past history of the regions.
 - Not Extinction but Attenuation
 - ▶ The reddening law was derived from measurements of stars, for which extinction occurs both by absorption and scattering all along the line of sight.
 - ▶ However, in AGNs, dust absorbs and scatters light, and scattering not only removes photons from the beam toward the observer, it also adds photons to it that were originally going in other directions.
 - ▶ In spherically symmetric systems, scattering within the line-emitting region has no effect, only the absorption effect would occur.
 - Clumpiness
 - ▶ In nearly all observed nebulae, the gas and dust have clumpy, irregular distributions.
 - Using one extinction law is an extreme oversimplification. The only justification is that at present we do not have sufficient information on the observed strengths of emission lines from AGNs.

-
- Diagnostic information on the physical conditions in the ionized gas in Cyg A.
 - Temperature
 - ▶ $[\text{O III}] (\lambda 4959 + \lambda 5007)/\lambda 4363 = 77$ gives $T = (1.5 \pm 0.1) \times 10^4 \text{ K}$ in the [O III] emitting region in the low-density limit ($n_e < 10^4 \text{ cm}^{-3}$) or lower temperature at higher electron density.
 - ▶ $[\text{N II}] (\lambda 6548 + \lambda 6583)/\lambda 5757 = 89$ corresponds to $T = 1.0 \times 10^4 \text{ K}$ in the low-density limit.
 - Density
 - ▶ $[\text{O III}] \lambda 3729/\lambda 3726$ is a good electron-density diagnostic in H II regions and PNe. However, this ratio cannot be applied in AGNs because their line widths are comparable to or larger than the separation of the two lines (2.8\AA , corresponding to $\sim 300 \text{ km s}^{-1}$).
 - ▶ $[\text{S II}] \lambda 6716/\lambda 6731 = 1.10$ corresponds to $n_E = 3 \times 10^2 \text{ cm}^{-3}$ at $T = 1.0 \times 10^4 \text{ K}$, or to $n_e = 4 \times 10^2 \text{ cm}^{-3}$ at $T = 1.5 \times 10^4 \text{ K}$.
 - ▶ [S II] emission arises in a less highly ionized region outside the [O III] emitting zone. Thus, the electron density derived from this ratio is not representative of the entire ionized volume. But, it seems unlikely that $n_e > 10^4 \text{ cm}^{-3}$.
 - Abundances
 - ▶ Assumes (1) $T = 8,500 \text{ K}$ for the [S III], [O I], and [N II] emitting regions, (2) $T = 12,000 \text{ K}$ for H I, He II, and He II, (3) $T = 15,000 \text{ K}$ for [O III] and [Ne III], (4) $T = 20,000 \text{ K}$ for [Ne V] and [Fe VII]

- ▶ The derived ionic abundances are shown in Table 13.3.
- ▶ With a rough allowance for unobserved stages of ionization, these ionic abundances give the approximate elemental abundances shown in Table 13.4.
- ▶ Table 13.4 shows that Cyg A has approximately the same composition as in our Galaxy and other observed galaxies with H II regions or starburst nuclei.
- ▶ H is the most abundant element; He is less abundant by a factor of ~ 10 ; O, Ne, N, and C are the most abundant heavy elements.
- ▶ Fe is underabundant, which can be understood as due to depletion onto grains, suggesting the existence of dust within the ionized gas.
- ▶ These abundances are useful as a starting point for model calculations based on a more specific physical model.

Table 13.3

Relative ionic composition of Cyg A emission-line region

| Ion | Abundance | Ion | Abundance |
|------------------|-------------------|------------------|--------------|
| H^+ | 10^4 | O^0 | 1.9 |
| He^+ | 5.7×10^2 | O^+ | 1.7 |
| He^{++} | 2.4×10^2 | O^{++} | 1.5 |
| N^0 | 0.37 | Ne^{++} | 0.45 |
| N^+ | 0.88 | Ne^{+4} | 0.16 |
| | | Fe^{+6} | ≤ 0.008 |

Table 13.4

Approximate elemental abundances in Cyg A emission-line region

| Element | Abundance | Element | Abundance |
|---------|-----------|---------|------------|
| H | 10^4 | Ne | 1 |
| He | 10^3 | S | 0.3 |
| N | 1 | Fe | ≤ 0.1 |
| O | 4 | | |

-
- Similar observational data are available for many other NLRGs and Seyfert 2 galaxies.
 - Table 13.5 gives a list of mean values of T and n_e determined from the best fits to [O III], [N II], [O II], [S II], and [O I] line ratios in Seyfert 2 and NLRGs.

[Table 13.5] Mean temperatures, electron densities, and extinctions in Seyfert 2 and NLRGs

| Galaxy | $\log T$ (K) | $\log n_e$ (cm^{-3}) | $E(B - V)$ |
|---------|--------------|---------------------------------|------------|
| Mrk 3 | 4.1 | 3.5 | 0.50 |
| Mrk 34 | 4.1 | 3.2 | 0.30 |
| Mrk 78 | 4.0 | 3.2 | 0.72 |
| Mrk 198 | 4.1 | 2.6 | 0.24 |
| Mrk 348 | 4.2 | 3.3 | 0.41 |
| 3C 33 | 4.1 | 2.9 | 0.38 |
| 3C 98 | 4.3 | 3.6 | 0.68 |
| 3C 327 | 4.3 | 3.2 | 0.43 |
| 3C 433 | 4.2 | 2.4 | 0.58 |

13.5 Photoionization

- Photoionization is the main ionization mechanism.
 - The temperature in the ionized gas in Cyg A and other NLRGs and Seyfert 2 galaxies $\sim 1 - 2 \times 10^4$ K.
 - In some Seyfert 2s and NLRGs, $[\text{O III}] (\lambda 4959 + \lambda 5007)/\lambda 4363$ is smaller, indicating higher temperature (up to $T \approx 5 \times 10^4$ K in some objects) and $n_e < 10^4 \text{ cm}^{-3}$, or $T \approx 1 - 2 \times 10^4$ K and higher densities (up to $n_e \approx 10^7 \text{ cm}^{-3}$).
 - These results strongly indicate that the main source of energy input is by photoionization.
 - **Under photoionization conditions, there is no direct relationship between gas temperature and degree of ionization.**
 - The radiative cooling by collisionally excited line radiation increases rapidly with increasing temperature, and this tends keep temperature $T \approx 1 - 2 \times 10^4$ K over a wide range of input ionization radiation spectra.
- Shock-wave heating?
 - **Under pure shock-wave (or collisional) heating, there is a direct relationship between temperature and degree of ionization**, and the [O III] lines would be radiated mostly at $T > 5 \times 10^4$ K.
 - In actual cases of shock-wave heating, pre-heating ahead of the shock front due to photoionization by radiation from the very hot gas close to the front. In this case, the [O III] emitting zone in shock gas always has $T > 3 \times 10^4$ K.
- The observations indicates that photoionization is operative in all (or most) AGNs, since the [O III] line ratios cannot be caused by collisional ionization.

-
- Ionization source with “Hard” spectrum
 - This simple analysis strongly implies that photoionization is the main energy-input mechanism.
 - However, it is clear that the main source of the radiation cannot be hot stars, as in H II regions and PNe. Radiation from such stars will not produce the wide range of ionization observed in NLRG and Seyfert 2 AGNs (emission lines of low stages [O I] and [S II], and high stages [Ne V] and [Fe VII])
 - What is required is a source with a much “harder” spectrum, that extends even further into the UV than the spectra of central stars of PNe, some of which have effective temperature up to $T = 2 \times 10^5$ K.
 - High-energy photons ($h\nu > 100$ eV) produce **high ionization (up to Ne^{+4} , Fe^{+6} , and even Fe^{+9}) near the source**, and **a long, partially-ionized “transition zone”** in which H^0 and H^+ , O^0 , and S^+ all coexist, and strong [O I] and [S II] lines can be collisionally excited.
 - The width of this transition zone is roughly one mean free path of an ionizing photon,

$$l = \frac{1}{n(\text{H}^0)\sigma_{\nu}^{\text{pi}}(\text{H}^0)}$$

Since both $n(\text{H}^0)$ and the mean frequency of the remaining photons vary rapidly with distance, the mean free path also varies rapidly.

The higher the energy of the photons present, the longer their mean free path is, and the larger the transition zone is.

- Spectral Energy Distributions (SEDs) of AGNs
 - A featureless continuum, extending across a broad range wavelengths, is observed in AGNs. The form of the SED in the optical-UV region approximately fits a power law:

$$L_\nu = C\nu^{-\alpha}$$
, typically with $\alpha \approx 1 - 2$.
 - In Cyg A, the “observed” continuum has $\alpha = 3.8$. But, if it is corrected for the same amount of extinction as derived from the Balmer decrement, this becomes $\alpha = 1.6$.
 - If this spectrum extended to high energies, its can explain the observed Cyg A line spectrum.

